Geology and geochronology of Monte de Trigo island alkaline suite, southeastern Brazil

Gaston Eduardo Rojas Enrich[1], Excelso Ruberti[2] & Celso de Barros Gomes[2]

Abstract The undersaturated syenite-gabbroid alkaline suite of Monte de Trigo Island lies in the northern sector of the Serra do Mar Alkaline Province in southeastern Brazil, and intrudes Precambrian gneissic and migmatitic rocks of the Ribeira Belt. It is made up by a cumulate mafic-ultramafic body, dominantly showing nepheline-bearing olivine melagabbros, melatheralites and clinopyroxenites, in association with synplutonic microtheralite and microessexite dykes, and by a miaskitic nepheline syenite stock genetically related to nepheline microsyenite dykes of miaskitic and agpaitic affinity. A magmatic breccia pipe having fragments derived from the mafic-ultramafic body and from the Precambrian country-rocks crops out in the eastern side of the island. The last magmatic alkaline event is represented by a series of lamprophyre-to-phonolite dykes. Geological evidences suggest a low emplacement level for the Monte de Trigo Island intrusion. Ar-Ar geochronological data for the different rock types yielded an average value of 86.6 Ma (Late Cretaceous), which is comparable to the age of other alkaline intrusions occurring in the northern sector of the Serra do Mar Province. The alkaline magmatism probably took place in a short time interval, lower than 0.5 Ma. Moreover, age incompatibility makes difficult to support the Trindade mantle plume model proposed for its origin. Thus, other factors such as pressure release and the influence of volatile phases in the source region might have contributed to the generation of the alkaline magmas.

Keywords: alkaline rocks, Serra do Mar Province, Ar-Ar geochronology.

Resumo *Geologia e geocronologia da suíte alcalina da ilha Monte de Trigo, sudeste do Brasil.* A suíte alcalina insaturada sienítica-gabróide da Ilha Monte de Trigo, localizada no setor norte da Província da Serra do Mar, está encaixada em rochas gnáissicas e migmatíticas pré-cambrianas da Faixa Ribeira. Ela consiste em um corpo máfico-ultramáfico cumulático, onde predominam olivina melagabros com nefelina, melateralitos e clinopiroxenitos associados a diques sin-plutônicos de microteralito e microessexito, e um *stock* de nefelina sienito geneticamente relacionado com diques de nefelina microssienito de afinidade miaskítica e agpaítica. Um *pipe* de brecha magmática, contendo fragmentos derivados do corpo máfico-ultramáfico e das rochas encaixantes pré-cambrianas, aflora na parte leste da ilha. A última atividade magmática alcalina é representada por uma série de diques variando composicionalmente de lamprófiros a fonólitos. Evidências geológicas sugerem que a colocação da intrusão de Monte de Trigo se deu em profundidade rasa. Resultados geocronológicos de Ar-Ar para diferentes litologias da ilha forneceram uma idade média de 86,6 Ma (Cretáceo Superior), que é comparável à idade dos demais corpos alcalinos do setor norte da Província Serra do Mar. O magmatismo se deu num curto intervalo de tempo, inferior a 0,5 Ma. Além disso, a incompatibilidade de idades torna difícil a aceitação do modelo da pluma de Trindade proposto para a sua origem. Assim, outros fatores como a despressurização e a presença de fases voláteis na fonte devem ter contribuído para a geração dos magmas alcalinos.

Palavras-chave: rochas alcalinas, Província Serra do Mar, geocronologia Ar-Ar.

INTRODUCTION Several alkaline rock occurrences lie in the northern coast of São Paulo State. They include the syenitic intrusions of São Sebastião (Mirante, São Sebastião and Serraria stocks), Búzios, Vitória and Monte de Trigo, among minor mafic cumulatic bodies and lamprophyric dykes, mostly described in the middle of the last century (Freitas 1947, Björnberg & Ellert 1955, Gomes *et al.* 1967).

The Monte de Trigo alkaline suite was first geologically and petrographically described by Coutinho & Melcher (1973), although they covered only a small part of the island. Other papers leading to a better geological knowledge of the island were the K-Ar geochronological work by Amaral *et al.* (1967) and the geochemical investigation of three mafic dykes, with a brief petrographic description, by Thompson *et al.* (1998).

This paper aims to provide a complete description of the alkaline suite and to discuss its magmatic evolution within a regional and geochronological context. It brings a detailed geologic map of the island, with emphasis on the characterization and geographic distribution of the main rock types as well as new $^{40}Ar/^{39}Ar$ ages on biotites and amphiboles.

1 - Programa de Pós-Graduação, Instituto de Geociências, São Paulo (SP), Brazil. E-mail: gastonenrich@usp.br
2 - Universidade de São Paulo, Instituto de Geociências, São Paulo (SP), Brazil. E-mail: exrubert@usp.br; cgomes@usp.br

REGIONAL CONTEXT A great number of alkaline and alkaline-carbonatite occurrences crop out at the borders of the Paraná Basin in the central-southeastern part of the Brazilian Platform (Ulbrich & Gomes 1981, Gomes *et al*. 1990, Morbidelli *et al*. 1995, Comin-Chiaramonti & Gomes 2005). They cover a large span of age, from Permo-Triassic to Paleogene (250-50 Ma), but only a few chronogroups are distinguished (Amaral *et al.* 1967, Ulbrich *et al.* 1991, Comin-Chiaramonti & Gomes 2005). Almeida (1983) grouped the several occurrences into various alkaline provinces, which have been more recently reviewed by Riccomini *et al.* (2005), mainly on the basis of tectonic and geochronological evidence. These authors proposed to assemble the numerous occurrences into fifteen distinct provinces.

Five out of that total are Late Cretaceous in age: Piratini, Serra do Mar, Cabo Frio Magmatic Lineament, Minas-Goiás and Rondonópolis Anteclise. Particularly, the Serra do Mar intrusions lie in the onshore continental region at the western borders of the Santos Basin and extend over nearly 650 km of the Brazilian southeastern coast. Moreover, the latter authors further subdivided the Serra do Mar Province into three sectors - northern, central and southern -, which are related to areas of major Cenozoic uplift.

The Monte de Trigo Island lies in the northern sector of the Serra do Mar Province (Fig. 1), also including the syenitic stocks of São Sebastião (Freitas 1947, Hennies & Hasui 1977, Bellieni *et al*. 1990, Enrich *et al.* 2005), Vitória (Gomes *et al.* 1967, Motoki & Gomes 1984) and Búzios (Björnberg & Ellert 1955, Alves & Gomes 2001) islands. Stocks are usually zoned, with borders of alkali feldspar syenites or quartz-bearing alkali feldspar syenites and cores of syenites or nepheline syenites. Mafic rock types are represented by cumulate bodies, similar to those found in the São Sebastião Island (Lima 2001, Augusto & Vlach inédito, Enrich *et al.* 2005) or in the Ponte Nova complex (Azzone *et al.* 2004), and by lamprophyric dyke swarms spreading over the whole region (Coutinho & Ens 1992, Garda *et al.* 1995, Garda & Schorscher 1996, Thompson *et al.* 1998).

The Serra do Mar alkaline rocks are emplaced into a Precambrian basement (Ribeira belt, 750-450 Ma; Machado *et al.* 1996, Heilbron *et al.* 2004) and they have K-Ar and Rb-Sr ages ranging from 80 to 90 Ma, most data being in the 81-86 Ma interval (Amaral *et al.* 1967, Sonoki & Garda 1988, Bellieni *et al.* 1990, Montes Lauar *et al.* 1995, Alves & Gomes 2001).

GEOLOGY Monte de Trigo (23°53'S, 45°47'W) is a small, ellipse-shaped island, 1.3 km^2 in area and 289 m high (Figs. 2, 3A), located about 10 km away from the continental area (Barra do Una beach) and, from the morphological point of view, clearly conditioned by N40W and N50E lineaments.

The alkaline rocks are delimited by the coastline, without an *in-situ* outcrop of the Precambrian country-rocks. They intrude gneisses and migmatites, as suggested by the presence of some rounded blocks (up to 1 m in diameter) within the northern coast of the island and also in the interior of the magmatic breccia pipe. This geological evidence is in agreement with the regional geomorphologic evolution proposed by Almeida & Carneiro (1998) that extends the ancient border of the Serra do Mar mountain range to the Santos fault, and places the Monte de Trigo magmatism under the Planalto Atlântico (Atlantic Plateau).

The alkaline magmatism is represented by silica-undersaturated rocks of syenite-gabbroid filiation (Fig. 2), characterizing four distinct episodes of activ-

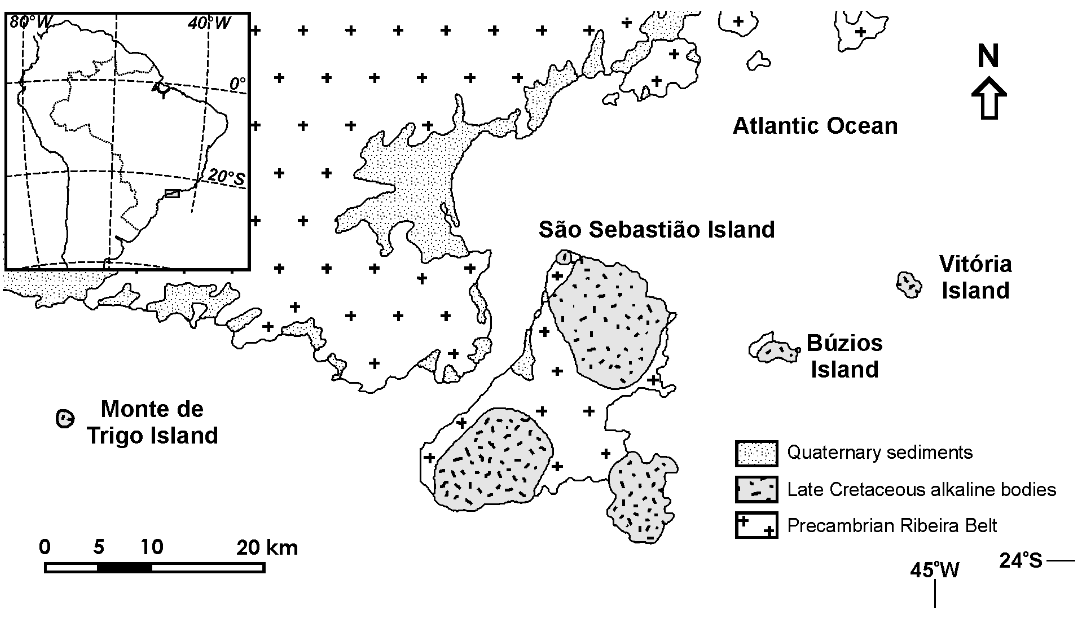

Figure 1 - Geological map of the northern sector of the Serra do Mar Alkaline Province, excluded the Ponte Nova occurrence.

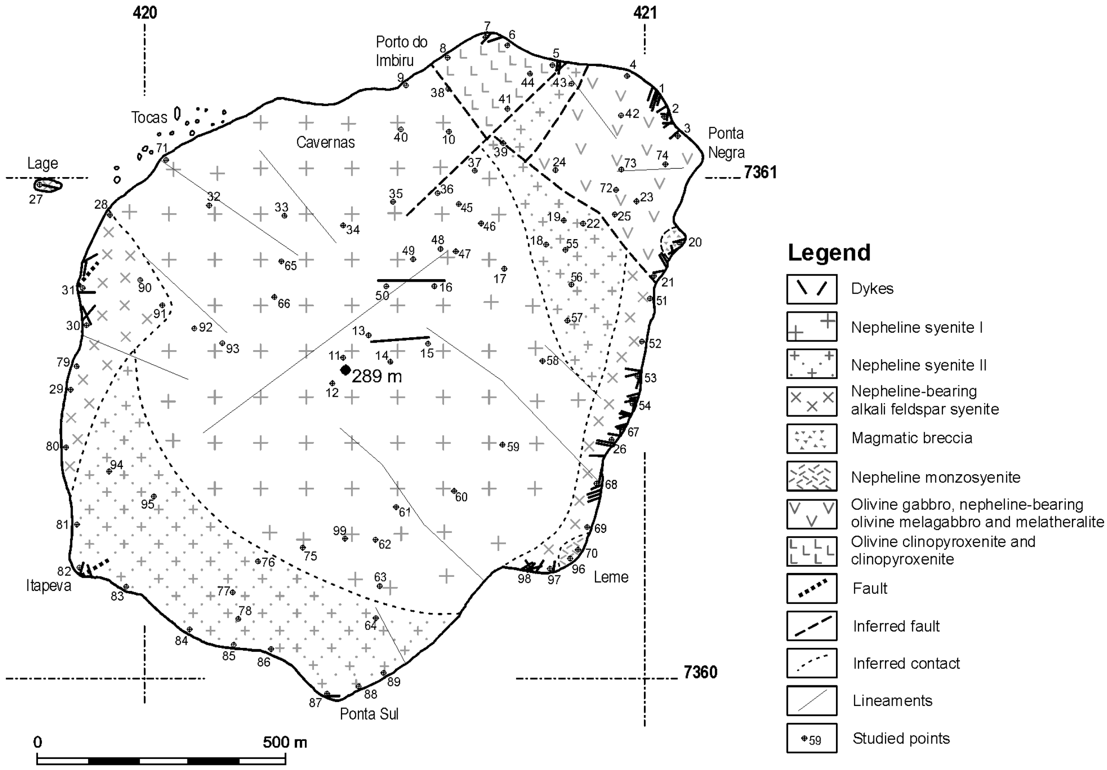

Figure 2 - Geological map of the Monte de Trigo Island alkaline suite.

ity: 1) an intrusive mafic-ultramafic body; 2) a breccia pipe; 3) an intrusive nepheline syenite stock; and 4) a series of lamprophyre to phonolite dykes. Hololeucocratic to ultramafic lithologies show a large mineralogical variety, being distinguished almost fifty different phases. Geomorphologic lineaments are suggestive of tectonic contacts between the nepheline syenite stock and the mafic-ultramafic body.

The cumulate mafic-ultramafic association is believed to be the oldest magmatic activity in Monte de Trigo. Three distinct facies were recognized, the first one being of mafic composition and found at the northeast part of the island. It is represented by theralites, melatheralites and nepheline-bearing olivine melagabbros displaying local variations to olivine gabbros at the northeastern edge. The second facies is clearly ultramafic, with clinopyroxenites and olivine clinopyroxenites cropping out at the northern tip of the island. Blocks of theralite and nepheline monzosyenite are also present at the southeastern edge, next to Leme. These blocks of nepheline monzosyenite represent the third facies. Moreover, microtheralite and microessexite synplutonic dykes of sinuous form, decimeter-scale thick and NE-SW preferential orientation complete the magmatic episode cutting the above-mentioned facies.

Theralites and gabbros may contain layered structures (Figs. 3B, C), up to 3 m wide, with each strata, compositionally felsic or mafic, varying from 5 to 20 cm. Sometimes they exhibit channel form or discordant pattern (e.g. crusade bedding). ENE-WSW strike and vertical dipping are predominant at northwest of Ponta Negra, but in the northeastern area of the island the orientation shifts to NW-SE. These features are comparable to the trough band or trough layer structures described in the localities of Skaergaard (Wager & Brown 1968), Fiskenaesset (Myers 1976) and Kokklen (Parson & Becker 1987).

The second magmatic activity is represented by an intrusive breccia pipe (about 50 to 60 m in diameter) cutting olivine gabbros and cropping out at south of Ponta Negra. Small-brecciated dykes (<50 cm) also occur. The main breccia body shows four different facies (Fig. 4). Facies I is matrix-supported, with rounded fragments, 1.0 mm to 1.1 m in diameter, of gneiss and migmatite associated with a gray matrix, aphanitic to fine-grained in size (Fig. 3D). Facies II is fragment-supported, with partial rounded gabbroic, theralitic and pyroxenitic fragments, up to 2 m in diameter. Smaller and more rounded migmatite fragments are subordinate. It shows a heterogeneous sulfide-rich matrix, aphanitic to fine-grained, widely variable in color suggesting assimilation of fragments. Facies III differs from II due to the presence of miarolitic cavities up to 10 cm wide, filled by sulfide, carbonates and zeolites. A pronounced decrease in the amount of basement rocks fragments is also noted. Facies IV is fragment-supported, prevailing clinopyroxenite and olivine clinopyroxenite fragments. Miarolitic cavities and migmatite-gneiss fragments are practically absent.

The third magmatic phase is represented by a nepheline syenite and nepheline-bearing alkali feldspar syenite stock associated with synplutonic nepheline microsyenite

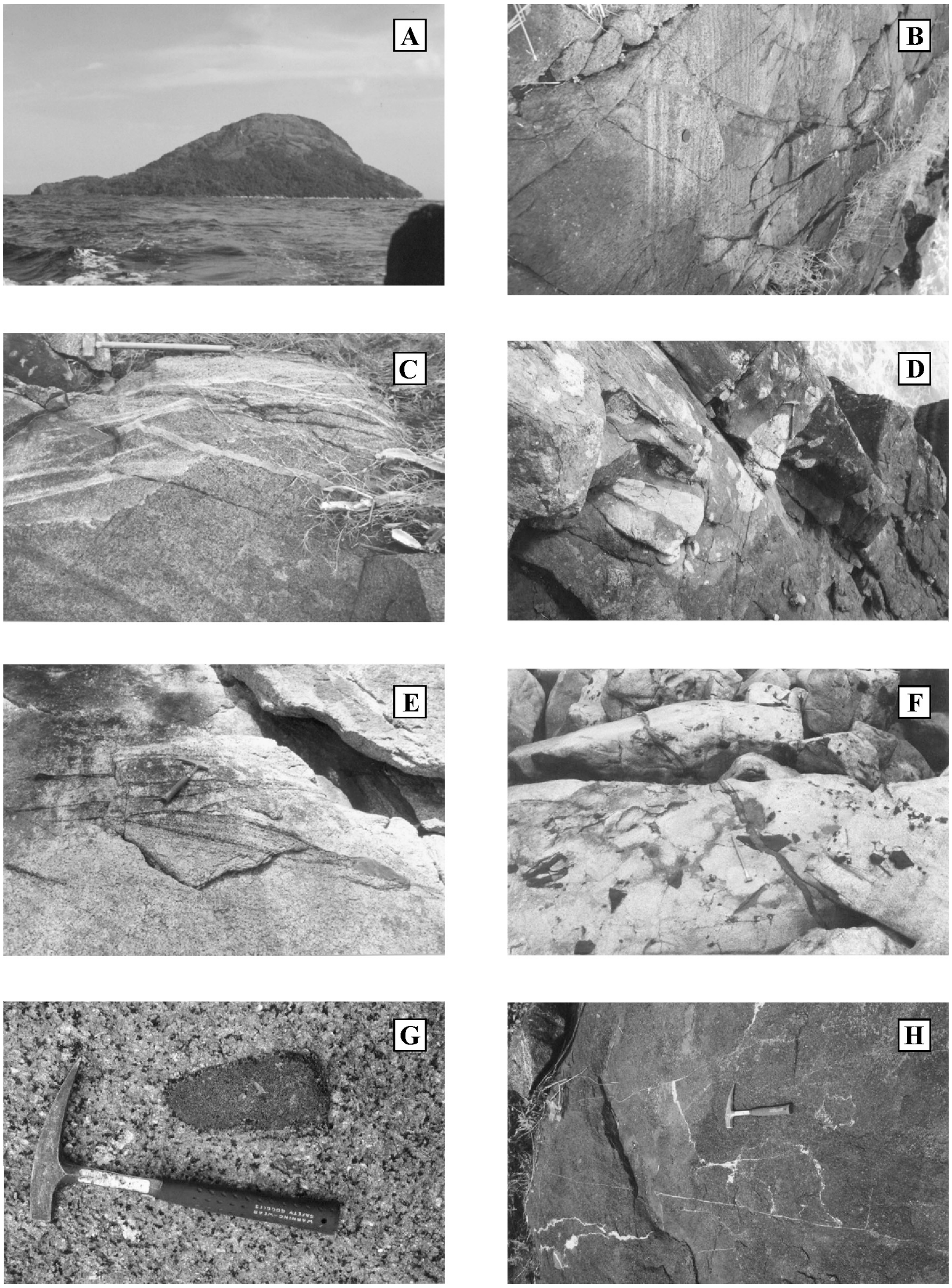

Figure 3 - (A) General view of the island northern side. (B) Layered structure, vertically dipping, in olivine gabbros near to the contact with nepheline-bearing alkali feldspar syenites. (C) Outcrop details of layered and massive olivine gabbros, both facies being cutted by a microtheralite dyke (lighter). (D) Rounded fragments of gneiss and migmatite in the magmatic breccia (Facie I). (E) Mafic layering in nepheline-bearing alkali feldspar syenites. (F) Several angular nepheline-bearing melagabbro xenoliths within the nepheline-bearing alkali feldspar syenites, near Leme. (G) Mafic enclave in nepheline-bearing alkali feldspar syenites. (H) Felsic veinlets within the adcumulatic clinopyroxenites, near Imbiru.

dykes. These rock types are dominant and are mainly concentrated in the central-southern area of the island.

The stock is formed by three distinct miaskitic facies of approximately concentric distribution (Fig. 2). Nepheline syenites I are the most undersaturated facies and occupy the central region. Nepheline syenites II surround the previous rocks from Ponta do Itapeva to Leme in the south and, along the contact with olivine gabbros, olivine (mela) gabbros with nepheline and (mela) theralites, in the northeast. The nepheline-bearing alkali feldspar syenites occur along the coastline, both in the east, between Lage and Ponta do Itapeva, and in the west, between Ponta Negra and Leme. The geological contact among the different facies is roughly estimated, being probably gradual in some places.

Layered structures are occasionally present, mostly in the nepheline-bearing alkali feldspar syenites (Fig. 3E). The most expressive occurrence is located in the east coast, next to the contact with the mafic body. There, some blocks display a band sequence that alternates, at each 10 cm, a mafic mineral association varying in volume of 15 to 30%. Other layered occurrences were recognized not far from the north of the island and along its west coast, showing vertical dipping and sinuous channel-like layers, respectively.

Hundreds of angular xenoliths are found within the nepheline-bearing alkali feldspar syenites (Fig. 3F) between Leme and Ponta Sul. They have millimeter- to meter-scale and are mainly composed of porphyritic nepheline-bearing melagabbros with a fine matrix, likely the rock types belonging to the first magmatic phase. In general, they do not exhibit any evidence of assimilation. Locally, it is also possible to distinguish two types of nepheline-bearing alkali feldspar syenites, one carrying xenoliths and the other being xenoliths-free.

Nepheline-bearing alkali feldspar syenites also have rounded mesocratic microgranular enclaves, up to 15 cm in diameter (Fig. 3G), displaying amphibole-rich borders and feldspar phenocrysts.

Miaskitic and agpaitic nepheline microsyenite dykes cut all the previous described rocks, although they are more commonly associated with nepheline-bearing alkali feldspar syenites. These dykes are up to 1 m wide, with slightly sinuous walls and do not show cooling edges, thus suggesting a synplutonic relationship. Some porphyritic varieties have tabular phenocrysts of alkali feldspar oriented according to the dyke direction. Pegmatite portions at the center of one dyke are also found.

Reaction bands were usually recognized at the contact between agpaitic nepheline microsyenite dykes and cumulate mafic-ultramafic rocks. They are up to 10 cm wide and display fine-grained texture and greenish tones. Moreover, drop-like corroded xenoliths of mafic-ultramafic rocks, found inside one of those dykes, exhibit an orientation suggestive of horizontal magmatic flow from south to north (cf. Rickwood 1990), i.e. with the magma coming from the direction of the nepheline syenitic stock.

The fourth magmatic phase is represented by a series of porphyritic dykes of aphanitic groundmass. It includes lamprophyres (monchiquite and camptonite), tephrites, phonolitic tephrites, tephritic phonolites and phonolites. Dykes are vertical, 5 cm to 2 m thick, and intrude all the additional intrusive rocks with straight contacts and chilled margins; some of them showing bridge or overlap structures. They usually occur as a small dyke set (Fig. 2), preferentially following E-W and NW-SE strikes (Fig. 5). In general, the felsic dykes (phonolite and tephritic phonolite) cut the mafic ones (lamprophyre, tephrite and phonolitic tephrite). A brecciated lamprophyre dyke was also found next to Leme.

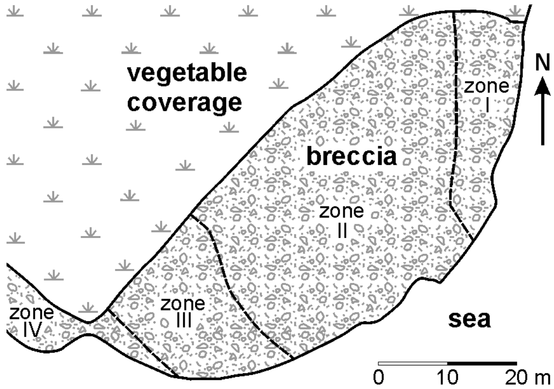

Figure 4 - Geological sketch-map of the magmatic breccia located at point 20 of Fig. 2.

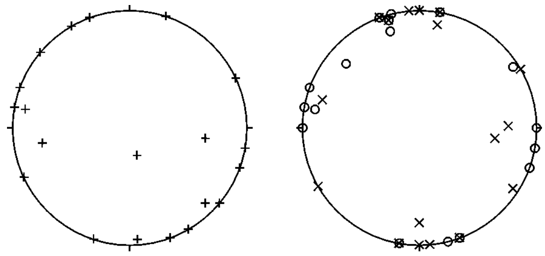

Figure 5 - Equal-area stereographic projections (lower hemisphere) of poles to the island dykes.

It is about 7.5 m thick and includes several rounded xenoliths, up to 30 cm in diameter, of nepheline syenites.

Two major NE-SW shear zones, i.e. parallel to the morphological lineaments, intersect the massif. The first one, about 10 m thick, is located near Ponta do Itapeva and cuts nepheline syenites II and a phonolite dyke. The second, 2-3 m thick, is situated at the western coastline and crosses nepheline-bearing alkali feldspar syenites. It has a high concentration of biotite and amphibole, sometimes forming small breccias and boudins.

PETROGRAPHY Descriptions of plutonic facies and dykes are based on classical bibliography (Tröger 1979, Williams *et al.* 1982, Deer *et al.* 1992, Mackenzie *et al.* 1993) and rock classification follows to IUGS recommendations (Le Maitre 2002). Representative modal analyses of the main rock types are given in table 1. Additional modal data are found in Coutinho & Melcher (1973).

Olivine gabbros, nepheline-bearing olivine (mela) gabbros and (mela) theralites These rocks are massive, coarse- to medium-grained, melanocratic (M' 60-90) and typically inequigranular-seriate hypidiomorphic in texture, with scarce porphyritic and pegmatoid varieties. They are widely variable in modal composition

Table 1 - Modal mineralogical composition of representative rock types from the Monte de Trigo Island alkaline suite.

Lithology	olivine gabbro	nepheline-bearing olivine mela-gabbro	theralite	theralite	mela-theralite	clino-pyroxenite	olivine clino-pyroxenite	olivine clino-pyroxenite
Sample	MTR20I	MTR42A	MTR70B	MTR25A	MTR01D	MTR04B	MTR05C	MTR06A
pyroxene	38.7	50.3	31.5	26.7	55.5	61.3	63.2	65.5
olivine	14.2	7.7	3.1	13.1	11.7	1.1	16.5	7.3
opaques (magnetite)	7.5	3.7	3.2	4.0	5.8	10.5	1.9	8.2
amphibole	0.0	13.6	3.3	15.2	1.6	10.0	4.7	4.6
biotite	6.1	9.0	19.7	6.3	2.7	4.2	5.8	4.1
plagioclase	32.9	12.4	26.0	23.1	17.5	1.1	2.5	1.9
alkali feldspar	-	-	tr	-	-	-	-	-
nepheline	-	0.7	8.9	8.3	3.1	4.5	3.3	0.4
apatite	0.6	2.1	1.8	3.3	0.6	0.8	0.5	0.2
clorite/serpentine	-	-	0.6	-	1.4	-	-	4.1
carbonate	-	0.4	0.4	-	0.1	-	0.5	-
sericite/zeolite	-		-	-	-	-	0.1	3.7
muscovite	-	0.1	-	-	-	-	-	-
isotrope (analcime)	-	tr	1.5	-	tr	-	1.0	-
unidentified mesostases	-	-	-	-	-	6.5	-	-
total	100.0	100.0	100.0	100.0	100.0	100.0	100.0	100.0
M’	66.5	84.3	61.4	65.3	77.3	87.1	92.1	93.8

Lithology	nepheline monzosyenite	nepheline-bearing alkali feldspar syenite	alkali feldspar syenite	nepheline syenite II	nepheline syenite I	nepheline syenite I
Sample	MTR 70C	MTR 26C	MTR 31B	MTR 05E	MTR 15	MTR 41A
alkali feldspar	44.9	82.0	83.1	76.7	72.6	74.4
plagioclase	7.9	-	-	-	-	-
nepheline	25.3	0.2	0	5.2	14.1	6.8
amphibole	13.8	5.0	3.6	6.5	2.0	7.0
pyroxene	0.5	1.7	2.6	0.4	1.3	0.9
biotite	0.5	2.8	6.9	0.1	tr	-
opaques	0.7	0.9	0.9	0.6	0.9	0.9
titanite	-	-	0.3	tr	tr	tr
apatite	0.9	0.3	0.3	0.1	0.1	0.1
cancrinite	tr	1.5	1.0	2.5	4.2	2.7
analcime	2.5	1.9	0.4	3.5	3.7	5.1
muscovite	1.0	0.6	0.6	1.6	0.4	0.7
carbonate	0.2	0.2	0.2	0.3	0.1	0.9
limonite	1.6	2.3	tr	2.2	0.4	0.3
unidentified mesostases	-	0.5	tr	0.1	0.2	0.4
total	99.8	99.9	99.9	99.8	99.9	100.2
M’	17.1	12.7	14.3	9.8	4.6	9.1

(Tab. 1) and have diopside (27-56%) and plagioclase (12-33%) as main minerals. A slight eastward decrease in the M' index is observed along the northern coastline other than local variations to more felsic rocks.

Olivine (chrysolite-hyalosiderite) grains, euhedral to anhedral in shape, are early crystallized phases with thin opaque lamellae. Common alteration products include bowlingite, chlorophaeite, chlorite and opaque minerals.

Euhedral to subhedral diopside grains are frequently zoned (normal, oscillatory or convolute), prevailing grey to pale brown cores and pale pink borders. A few borders also contain inclusions of amphibole, magnetite and biotite cutting the magmatic zoning. Kaersutite and biotite are found as interstitial to poikilitic grains. Late biotite occurs along fractures or overgrowing magnetite grains.

Small plagioclase laths are present between clinopyroxene and olivine grains. They exhibit simple, step or oscillatory zoning and are dominantly of bytownite composition in the cores and labradorite to oligoclase at the rims. Nepheline is interstitial and a cloudy mesostasis of potassic feldspar, sodalite and other minerals is occasionally recognized. Cancrinite and seric ite+analcime+carbonate+zeolite aggregates are typical alteration products. At Leme, theralites also show an intergrowth of nepheline and antiperthite oligoclase as well as interstitial analcime and carbonate.

Accessory minerals are granular magnetite with ilmenite and pleonaste lamellae, prismatic apatite and scarce subhedral titanite.

Clinopyroxenites and olivine clinopyroxenites These rocks are massive, coarse-grained, dark-colored and more rarely have brecciated blocks of the same lithology. In general, the texture varies from orthocumulate, at the contact with mafic rocks, to adcumulate, a more frequent feature near Porto do Imbiru area.

Orthocumulate varieties are characterized by an inequigranular seriate texture. *Cumulus* crystals include euhedral olivine (chrysolite-hyalosiderite) with opaque lamellae and oscillatory-zoned pink diopside (titanaugite), similar to those described in nepheline-bearing olivine gabbros and theralites. Euhedral to anhedral magnetite grains with thin exsolved ilmenite and pleonaste lamellae occur interstitially to the previous minerals.

Cumulus phases are surrounded by a matrix composed of subhedral to anhedral small grains of the same minerals, together with interstitial to poikilitic plagioclase, nepheline and kaersutite. Intergrowth relationship suggests the replacement of clinopyroxene by amphibole. Biotite is less abundant and found encompassing magnetite crystals or as small interstitial grains. Prismatic apatite is also present.

Otherwise, adcumulate lithotypes are equigranular in texture, with closely associated subhedral to anhedral grains of olivine, clinopyroxene and magnetite. Intercumulus material, mainly consisting of anhedral plagioclase and nepheline, forms interstitial aggregates, small pockets, up to 15 cm wide, or interlaced veinlets like a stockwork (Fig. 3H). Minor amounts of interstitial kaersutite and biotite are also identified. Prismatic apatite occurs within felsic aggregates.

Microtheralite and microessexite dykes These rocks are massive to foliated, mesocratic and fine- to medium-grained. Less evolved varieties are hypidiomorphic to allotriomorphic in texture. They include rounded olivine (hyalosiderite), zoned diopside, with lighter cores and pale brown to pink borders, magnetite and kaersutite, as well as biotite and poikilitic nepheline as interstitial phases.

In more evolved varieties, prismatic amphibole (kaersutite-pargasite) is the dominant mafic mineral. Olivine is absent, whereas clinopyroxene occurs in small amounts, displaying pale green rims (diopside-hedenbergite). Magnetite occurs commonly associated with the other mafic phases and biotite is scarce. Plagioclase (andesine) and alkali feldspar are subhedral to anhedral. Nepheline, the most abundant feldspatoid, is subhedral to anhedral.

In addition to the main rock-type, this group also includes a few dykes showing variable compositions such as diabase (plagioclase, clinopyroxene and opaques) and nephelinite (olivine, clinopiroxene, nepheline and opaques).

Nepheline monzosyenites These rocks are massive, medium-grained, leucocratic (M'~18) and trachytic to hypidiomorphic in texture, with tabular to slightly rounded plagioclase grains. This mineral displays normal zoning and it is overgrown epitaxially by a thick and irregular border of mesoperthitic alkali feldspar.

Among the large alkali feldspar crystals, there are clusters of euhedral to subhedral nepheline and amphibole grains, although nepheline is also found as anhedral inclusions in alkali feldspars. Amphibole, the dominant mafic mineral, is strongly zoned, showing kaersutite to pargasite cores and hastingsite rims. Other ferromagnesian phases include anhedral inclusions of a light green clinopyroxene (hedenbergite) occupying the central parts of the amphibole grains as well as interstitial aegirine-augite and biotite. Accessory minerals are anhedral magnetite with ilmenite lamellae, usually associated with amphibole and nepheline aggregates, anhedral pyrite and prismatic apatite.

Post-magmatic paragenesis consists of cuneiform analcime, albite and muscovite in addition to hydroxide and carbonate aggregates originated after amphibole.

Nepheline-bearing alkali feldspar syenites This facies also includes local variations to alkali feldspar syenites and analcime-bearing alkali feldspar syenites. The rocks are massive, equigranular, coarse-grained, M' index varying between 10 and 15 and exhibit trachytic to hypidiomorphic texture.

Alkali feldspar grains are mesoperthitic, tabular, euhedral to anhedral and twinned according to Carlsbad law. Portions of the grains show homogeneous (criptoperthitic?) to microperthitic aspect, together with braid, string or film perthites. The last perthite type is more commonly recognized near crystallographic discontinuities such as boundaries, fractures or inclusions. Remaining parts of the grains have irregular patch perthites. Moreover, samples located near the Lage shear zone display almost complete exsolved grains, with deuteric chessboard perthites.

Nepheline often occurs as interstitial crystals or anhedral inclusions in alkali feldspars. Analcime is scarce and probably has tardi- to post-magmatic origin.

Mafic clusters among alkali feldspar grains are made of subhedral to anhedral biotite, greenish-brown amphibole and green clinopyroxene. Textural relationships suggest amphibole formation after clinopyroxene and biotite substitution. Biotite is also found as small euhedral inclusions in alkali feldspars.

Anhedral magnetite with ilmenite lamellae occurs within mafic clusters or as rounded inclusions in alkali feldspars. Prismatic, primary ilmenite grains semi-included in magnetite are rarely present. Euhedral to subhedral titanite is more abundant in layered rock types whereas euhedral apatite is found as inclusions in all other mineral phases.

Nepheline syenites I These rocks are massive, medium-grained, inequigranular seriate hypidiomorphic to trachytic in texture and have M' between 4 and 9.

Mesoperthitic alkali feldspar, showing exsolution textures similar to those described in the nepheline-bearing alkali feldspar syenites, is present as tabular, euhedral to subhedral grains. Nepheline mostly forms large interstitial and poikilitic crystals, but it also occurs as anhedral inclusions in alkali feldspars. Its modal proportion varies between 5 and 15% in volume, the highest proportions found in rocks cropping out in the center (top) of the island.

Amphibole is the most abundant mafic mineral, forming isolated grains, euhedral to subhedral in shape, or small clusters. Its composition is variable, similar to the amphibole of nepheline syenite II. Hedenbergite occurs as euhedral to anhedral isolated grains or close to the borders of amphibole crystals, locally rimming it. Similarly to the nepheline it is more concentrated in rocks cropping out at the center of the island.

Granular magnetite with ilmenite lamellae is the main accessory mineral. It occurs in the interior or at the borders of clusters of mafic minerals, suggesting at least two distinct generations. Other accessories are prismatic to acicular apatite, anhedral titanite included in magnetite and amphibole grains and more rarely pyrite.

The post-magmatic paragenesis is similar to that of the nepheline syenites II and consists of analcime, albite and carbonate, together with alteration products of amphibole, clinopyroxene and nepheline.

Nepheline syenites II These rocks are massive, medium-grained, leucocratic (M' 7-10) and dominantly of inequigranular seriate hypidiomorphic texture; only locally the texture is trachytic.

Alkali feldspar is tabular to equidimensional, subhedral and mesoperthitic. It shows exsolution structures similar to those described in the nepheline-bearing alkali feldspar syenites facies. Nepheline (~5% vol.) is interstitial, but also found as anhedral inclusions in alkali feldspars.

Amphibole is the main mafic phase and forms clusters of euhedral to subhedral grains. Its composition varies from pargasite (greenish-brown, reddish-brown to yellow) in the central parts of the crystals to hastingsite (dark green to yellow) at the borders. Hedenbergite and biotite are only present as anhedral inclusions in amphiboles.

Rounded magnetite grains with ilmenite lamellae occur associated with amphibole clusters or as small grains inside the alkali feldspars. Other accessory minerals are euhedral apatite, anhedral titanite and scarce pyrite.

Grain interstices are partially filled by a post-magmatic paragenesis having cuneiform analcime with anomalous birefringence, albite and carbonate. The last phase is also present as euhedral inclusions in analcime. Moreover, amphibole and nepheline are replaced by mineralogical assemblages, mainly made of limonite+carbonate and analcime+cancrinite+muscovite+zeolite, respectively.

Miaskitic nepheline microsyenite dykes They are leucocratic, massive to foliated and fine- to medium-grained rocks. Inequigranular seriate texture prevails, with variations to trachytic, hypidiomorphic and allotriomorphic.

Mesoperthite alkali feldspar is granular to prismatic in shape. Frequently, portions of patch perthites exsolve the whole grain. Nepheline forms interstitial poikilitic grains, surrounding amphibole and feldspar, or clusters of subhedral granular crystals. Sodalite, with anhedral habit and turbid aspect, is present in some dykes. Analcime occurs as clear, interstitial and cuneiform-shaped grains, and exhibits anomalous birefringence.

The proportion of mafic minerals, particularly of clinopyroxene and amphibole, is quite variable. The most common clinopyroxene is a granular anhedral aegirine-augite, which frequently forms clusters and interstitial grains in the trachytic varieties. Subhedral to euhedral amphibole is also found as small interstitial clusters. Biotite is present in some samples as anhedral grains associated with amphibole. Magnetite is rounded in shape and in a few cases poikilitic with feldspar inclusions. Apatite, usually included in other phases, exhibits acicular to prismatic habit. Subhedral to euhedral titanite and prismatic to rounded zircon also occur. Other scarce accessory phases are sphalerite, pyrochlore, zirconolite and britholite.

Agpaitic nepheline microsyenite dykes They are hololeucocratic, inequigranular, fine- to medium-grained rocks and commonly allotriomorphic to hypidiomorphic in texture, although trachytic or aplitic varieties are also noted.

Alkali feldspar grains are mesoperthitic, subhedral, and have frequently rounded to prismatic shapes. Nepheline occurs as both euhedral and interstitial poikilitic grains, whereas sodalite and analcime are scarce.

Green clinopyroxene (aegirine to aegirine-augite) prevails among mafic minerals and forms isolated anhedral grains or clusters. Blueish-green amphibole is less abundant while biotite is rare. Rounded or poikilitic grains of mangano-magnetite with ilmenite or pyrophanite lamellae also occur.

Accessory phases include several rare minerals in different paragenesis at each sample, mostly identified by electron microprobe (unpublished data). Titanite and zircon form poikilitic to skeletal crystals, frequently associated with mangano-magnetite and small euhedral pyrochlore grains. Wöhlerite and hiortdahlite are widespread and show similar features. Both are light brown to colorless, usually present as subhedral prismatic to rounded crystals and occasionally zoned. Eudialyte is colorless, euhedral, hexagonal- to round-shaped, and exhibits low birefringence and moderate relief. Perovskite (loparite) is rarely found as anhedral (corroded?) inclusions in titanite, whereas britholite forms isolated anhedral grains. Apatite occurs after britholite or as isolated subhedral grains. Fluorite is scarce.

At the contact zone of the dykes, the anhydrous paragenesis (olivine, clinopyroxene, plagioclase, magnetite) of the mafic-ultramafic country-rock was replaced by a new mineralogical assemblage having amphibole, biotite, garnet, opaques and an unidentified felsic phase of the matrix (wollastonite or laarnite?). On the other hand, in the nepheline microsyenites, the presence of dark brown grains of prismatic zirconolite and acicular baddeleyite forming clusters with other mafic minerals and also låvenite as isolated anhedral crystals is recognized.

Monchiquite dykes These rocks are porphyritic to glomeroporphyritic and panidiomorphic in texture, having olivine and diopside phenocrysts. Occasionally, olivine exhibits skeletal texture and diopside oscillatory zoning and green cores. As suggested by Rock (1991), the last feature could be originated by the interaction of more differentiated magmas with new lamprophyric magma batches. Kaersutite phenocrysts are scarce and show embayment texture, suggestive of magmatic reabsorption before the matrix crystallization. Magnetite microphenocrysts are also present.

The matrix is micro- to cryptocrystalline, mainly composed of amphibole, magnetite and a fine groundmass, probably of altered devitrified glass. Carbonate-analcime globular structures are abundant within the matrix.

Camptonite dykes These rocks are panidiomorphic, with porphyritic to glomeroporphyritic texture and aphanitic to fine-grained matrix.

Zoned kaersutite phenocrysts prevail, with darker colors at the borders. Diopside phenocrysts display combined sector and oscillatory zoning. Some grains also show green cores like the monchiquites. Phenocrysts of anhedral olivine occur in small amounts and always in glomeroporphyritic arrangements, surrounded by clinopyroxene and amphibole grains.

Microcrystalline matrix is composed of an altered and poor-defined felsic groundmass. It is characterized by prismatic kaersutite and apatite, subhedral magnetite and feldspar, besides interstitial nepheline, sodalite and analcime. Some dykes have globular structures mostly constituted by carbonate and analcime.

Tephrite dykes These rocks are aphyric to porphyritic in texture and more rarely glomeroporphyritic with micro- to cryptocrystalline matrix.

In the porphyritic varieties, euhedral yellow to reddish orange kaersutite and zoned plagioclase, with labradorite cores, are the main phenocrysts, whereas euhedral to subhedral diopside-augite and clusters of euhedral magnetite occur subordinately. Small anhedral olivine grains form inclusions within the mafic phenocrysts.

The aphyric rocks and the matrix of the porphyritic varieties are composed of zoned prismatic amphibole, with red cores (probably kaersutite) and pale greenish-brown borders (probably hastingsite), anhedral green clinopyroxene (hedenbergite or aegirine-augite), tabular to poikilitic plagioclase, biotite, magnetite, apatite, cancrinite and isotropic minerals in addition to an interstitial felsic cryptocrystalline groundmass.

Phonolitic tephrite and tephritic phonolite dykes These rocks are aphyric or porphyritic in texture with aphanitic to fine-grained matrix.

In the porphyritic varieties, phenocrysts are mainly represented by prismatic zoned amphibole, showing yellow to reddish-orange cores (kaersutite or pargasite) and darker green rims (hastingsite). They are usually in contact with tabular plagioclase and mesoperthite alkali feldspar phenocrysts. Occasionally, subhedral biotite and zoned diopside-hedenbergite, with pink beige cores and green borders, occur as phenocrysts and anhedral clinopyroxene as inclusions in amphiboles. Microphenocrysts of euhedral magnetite are associated with the borders of amphibole crystals and apatite is found included in amphibole phenocrysts.

The aphyric rocks and the matrix of the porphyritic varieties have a pale green amphibole (probably hastingsite) as the prevailing mafic mineral. Green clinopyroxene (hedenbergite to aegirine-augite), brown biotite, magnetite and acicular apatite are also present. Mesoperthitic alkali feldspar and plagioclase are interstitial phases together with a fine felsic groundmass.

Phonolite dykes These rocks are leucocratic, porphyritic or glomeroporphyritic with a trachytic, fine-grained to aphanitic matrix. Flow textures are observed in some dykes due to the pronounced alignment of the phenocrysts.

Phenocrysts of mesoperthite alkali feldspar prevail. Zoned plagioclase grains with oligoclase cores are rarely found. Euhedral nepheline only occurs as phenocrysts in a few samples. Amphibole is restricted to varieties without nepheline phenocrysts. The amphibole is euhedral and exhibits reddish cores and dark brown borders. Biotite occurs in aggregates forming hexagonal pseudomorphs, together with apatite, zircon, analcime and cancrinite. In some cases, these pseudomorphs have aegirine-augite rims or relicts of diopside or titanaugite. Apatite and magnetite are present as inclusions in the amphiboles. Moreover, microphenocrysts of cancrinite, biotite, analcime and more rarely of clinopyroxene are found.

Aphyric varieties and the matrix of the porphyritic types are microcrystalline and made of small prisms of alkali feldspar and subhedral to interstitial grains of nepheline, cancrinite, aegirine-augite and biotite.

^{40}Ar/^{39}Ar AGE Biotite grains taken from different rock types (nepheline-bearing olivine gabbro, theralite, nepheline syenite II, nepheline-bearing alkali feldspar syenite and biotite lamprophyre) and an amphibole grain from a phonolite dyke were selected for geochronological studies. These lithologies are believed to represent the entire magmatic history of the island. The grains were analyzed by ^{40}Ar/^{39}Ar laser step-heating methods with a MAP-215 spectrometer at the Centro de Pesquisas Geocronológicas (CPGeo) of the Instituto de Geociências, University of São Paulo. Before the analyses, they were irradiated in the IEA-R1 nuclear reactor of the Instituto de Pesquisas Energéticas e Nucleares (IPEN). Analytical procedures are those described in Vasconcellos *et al.* (2002).

Table 2 lists the ^{40}Ar/^{39}Ar ages for the main Monte de Trigo Island rock types. In general, laser-heating steps provided excellent plateau ages on biotite grains (Fig. 6), with values very close to those of the integrated ages.

Biotite ^{40}Ar/^{39}Ar plateau ages yielded values varying from 86.1 to 87.2 Ma and an average age of 86.6 Ma. This short interval is within the analytical error of ±0.5 Ma, suggesting that apparently no age differences do exist among the samples. Furthermore, the integrated ages lie between 86.3 and 86.9 Ma, within the same analytical interval.

On the other hand, the amphibole from the peralkaline phonolite dyke, representing the youngest magmatic event in the island, shows plateau and integrated ages of 84.4±1.0 Ma and 86±1 Ma, respectively. However, the large error and the fact that the analysis was carried out in a different mineral due to the absence of well-formed biotite grains in the rock, put some constrains in any interpretation regarding the real meaning of that ages difference.

DISCUSSION AND FINAL REMARKS

Magmatic evolution Geological and petrographic data allow us to conclude that Precambrian rocks of the Ribeira Belt were intruded by successive and different pulses of undersaturated alkaline magmas in the Monte de Trigo Island. Age values for the different rock types indicated a magmatic interval lower than the analytical error, i.e., 0.5 Ma. The emplacement of the alkaline rocks in this region is clearly controlled by tectonics, as already emphasized by Almeida (1983), Almeida & Carneiro (1998), Alves & Gomes (2001) and Riccomini *et al.* (2005).

Apparently, the magmatism started with an alkaline mafic magma chamber that crystallized theralites, melatheralites, nepheline-bearing olivine melagabbros, olivine gabbros, nepheline monzosyenites, clinopyroxenites and olivine clinopyroxenites. This interpretation significantly differs from that proposed by Coutinho & Melcher (1973), which considers the syenite magmatism as an earlier activity in the complex evolution. The great modal variation and the presence of layering structures and cumulate textures suggest that these lithologies were formed by fractional crystallization processes. Textural relationships indicate an early crystallization of olivine and diopside, followed by magnetite and plagioclase. The accumulation of these minerals in the magma chamber led to the formation of olivine gabbro, olivine clinopyroxenite and clinopyroxenite *cumulatus*, in a similar way to that reported for the Skaergaard complex by Wager & Brown (1968) and McBirney (1996).

Biotite, amphibole, plagioclase and nepheline

Table 2 - ^{40}Ar/^{39}Ar ages of representative rock types from the Monte de Trigo Island alkaline suite.

sample	lithology	mineral	plateau age (Ma)	integrated age (Ma)
MTR42a	nepheline-bearing olivine gabbro	biotite	86.5±0.5	86.7±0.4
MTR70b	theralite	biotite	86.5±0.4	86.7±0.2
MTR80b	nepheline syenite	biotite	86.6±0.5	86.9±0.4
MTR26c	nepheline-bearing alkali feldspar syenite	biotite	86.1±0.4	86.3±0.4
MTR26c duplicate	nepheline-bearing alkali feldspar syenite	biotite	86.7±0.4	86.6±0.3
MTR53d	biotite lamprophyre	biotite	87.2±0.5	86.9±0.4
MTR16b	peralkaline phonolite	amphibole	84.4±1.0	86±1

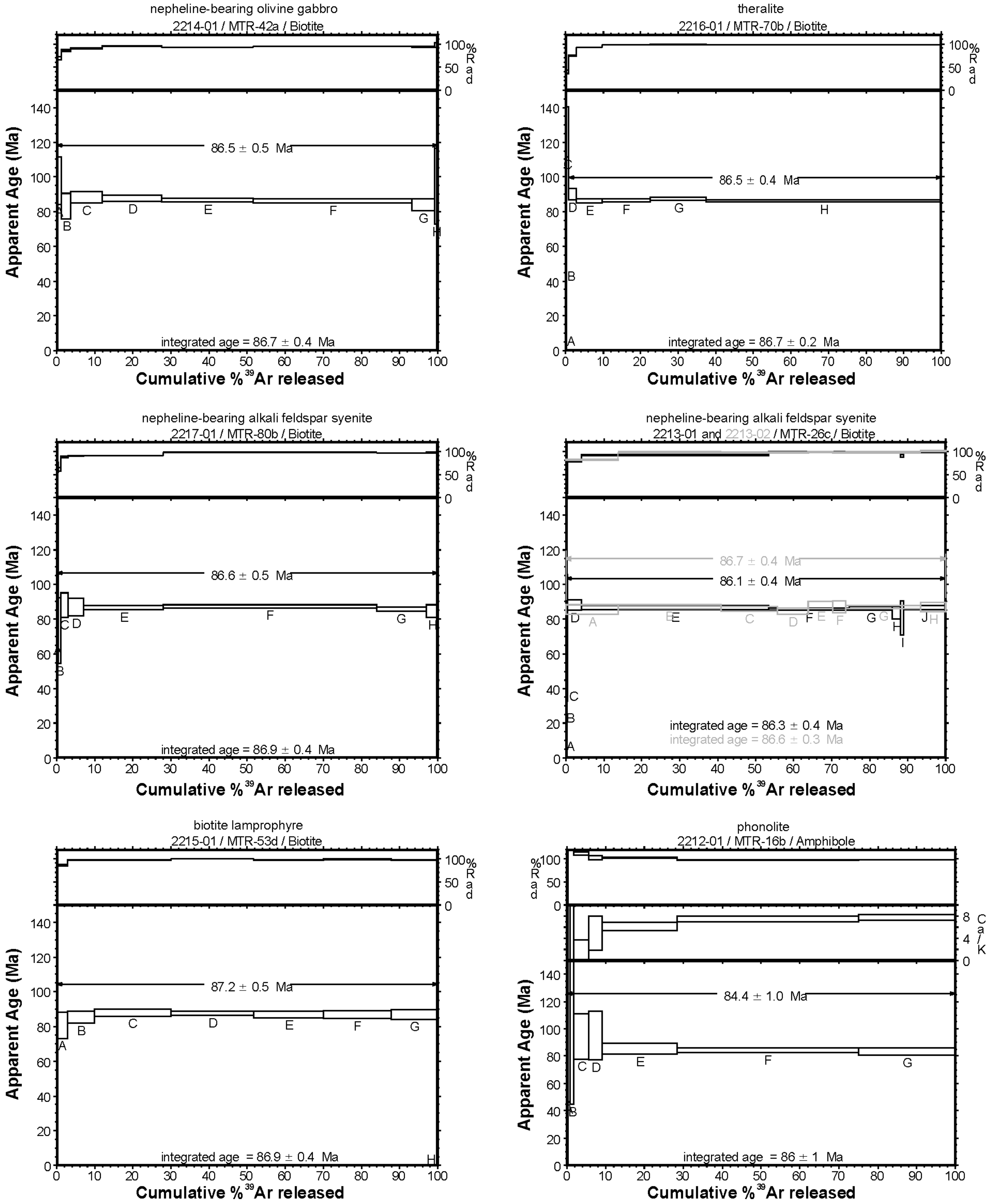

Figure 6 - $^{40}Ar/^{39}Ar$ step-heating (plateau) and integrated ages on biotite and amphibole from the Monte de Trigo Island rock types.

were formed interstitially to the cumulus minerals. In these rocks, the possibility of local migrations of intercumulus liquid to form veinlets or small pockets seems to be the cause of the main differences between adcumulatic and orthocumulatic varieties. Such differences could be the result of small variations in the compaction and local geometry, as well as of the influence of tectonic movements during crystallization. Microtheralite and microessexite dykes show a paragenesis comparable to the interstitial material and synplutonic relationships with the cumulatic rocks, suggesting that they represent their magmatic differentiate.

The available data make difficult to interpret the nepheline monzosyenites as a local differentiation product of the mafic-ultramafic rocks. Therefore, the genetic relationship is assumed based on its petrographic affinity and evolution coherence. The paragenesis of early crystallized minerals in nepheline monzosyenites (apatite, green clinopyroxene, plagioclase, magnetite and red-brown amphibole) is partially similar to that described for the intercumulus material and microtheralite and microessexite dykes. However, a marked change during the liquid evolution could lead to the crystallization of greenish to brown amphibole, nepheline and mesoperthitic alkali feldspar. In this case, the feldspar evolution is coherent with the "sequential two-feldspar paths*"* crystallization of Brown (1993).

The breccia emplacement represents the following magmatic phase. The presence of fragments of both Precambrian gneisses and migmatites and alkaline mafic-ultramafic rocks clearly indicates the proposed sequence, which is also confirmed by the absence of fragments of syenitic rocks, although they are found near to the breccia outcrops. Geological and petrographic relationships suggest that the breccia was formed by a volatile-rich alkaline mafic magma.

The next step in the petrologic evolution of the intrusion is represented by the nepheline syenite stock and its synplutonic dykes. The crystallization process starts with the accessory minerals apatite, magnetite and titanite, giving to the intrusion its miaskitic character. Amphibole, clinopyroxene and biotite crystallized during all magmatic history, although their mutual relationships are not clear. Alkali feldspar also crystallized during all magmatic history, whereas feldspathoids are usually late phases. Fractionation of alkali feldspar, together with the M' index variation, points to an evolution sequence from nepheline-bearing alkali feldspar syenites, at the borders of the stock, through nepheline syenites II and then to nepheline syenites I, at the center. Both agpaitic and miaskitic synplutonic nepheline microsyenite dykes are emplaced as final differentiates. This evolution is coherent with the quartz-nepheline-kalsilite residual system of Hamilton & Mackenzie (1965), evolving right through the undersaturated eutectic point.

The last alkaline magmatic manifestation of the island is a dyke series compositionally varying from lamprophryres to phonolites. Petrographic data suggest that they could be part of a single magmatic sequence, probably formed by the fractionation of the phenocrysts assemblage. These dykes were emplaced in a brittle fashion, suggesting low pressure conditions and relatively cold environment.

Overall, the alkaline magmatism of the Monte de Trigo Island is bimodal, with prevailing leucocratic and melanocratic-ultramafic lithologies. In fact, nepheline monzosyenites, phonolitic tephrites and tephritic phonolites are less abundant, and their origin could be linked to both fractional crystallization of mafic magmas or mixture between mafic and felsic melts. This aspect leads to a classic petrologic question regarding the alkaline rocks known as 'Daly gap' (Chayes 1977), which seems to be present in some occurrences of the region (e.g. Alves & Gomes 2001, Enrich *et al.* 2005).

Geodynamic context According to Gibson *et al.* (1995) and Thompson *et al.* (1998), Late Cretaceous alkaline occurrences in the Brazilian Platform are genetically associated with the presence of the Trindade mantle plume, whose impact on the north of the Paraná Basin would have produced the magmatism. However, the mantle plume hypothesis has been subject of a certain controversy (e.g. Comin-Chiaramonti *et al.* 2002, 2005) since it does not clearly explain the genesis and distribution of some Brazilian Late Cretaceous alkaline igneous centers, as those of Lages and Piratini in southern Brazil.

Specifically for the region encompassing the northern sector of Serra do Mar and Cabo Frio Magmatic Lineament provinces, Thompson *et al.* (1998) argued that the Trindade mantle plume was responsible for the genesis of alkaline melts. During the westward displacement of the continental platform, between ~80 and 55 Ma, the Trindade mantle plume would have migrated several hundred kilometers to a thinner lithosphere in the South, due to the presence of the São Francisco craton. In fact, this model could only explain the distribution in space and time of the alkaline magmatism along the Cabo Frio Magmatic Lineament, which is beyond the scope of this paper.

The Monte de Trigo age (86.6 Ma) as well as the ages of other occurrences lying in the northern sector of the Serra do Mar Province (81-86 Ma: Amaral *et al*. 1967, Sonoki & Garda 1988, Bellieni *et al.* 1990, Montes Lauar *et al.* 1995, Alves & Gomes 2001) are not compatible with the Trindade mantle plume hypothesis. Moreover, the estimated distance of ~1000 km from these bodies to the plume axis, separated by the thicker lithosphere of the São Francisco craton, does not support the influence of the plume on their genesis.

Alternatively, Smith & Lewis (1999) and Comin-Chiaramonti *et al.* (2005) proposed that pressure release together with rifting associated with South American plate movements and the presence of volatile phases in the mantle (*wet spot*) are the major agents responsible for the generation of alkaline magmatism and its distribution in space and time. Additionally, a possibly higher temperature could be the result of a regional thermal anomaly (Ernesto *et al.* 2002) or of a residual heating from the Early Cretaceous Tristan da Cunha mantle plume (Vandercar *et al.* 1995).

Therefore, it is suggested that pressure release associated with the presence of volatile phases in the lithospheric mantle would have produced the Monte de Trigo alkaline magmatism and its neighbor occurrences, in conformity to the hypothesis of Smith & Lewis (1999) and Comin-Chiaramonti *et al.* (2005).

Acknowledgments This research was supported by FAPESP (Procs. 00/12576-4 and 01/10714-3). Thanks are due to Artur Deodato Alves, Willian Salun Filho, Artur Vinha Fosse and Jaime Presser for their valuable assistance during the fieldwork. Further thanks go to Artur Takashi Onoe for the Ar-Ar analyses.

References

Almeida F.F.M. 1983. Relações tectônicas das rochas alcalinas mesozóicas da região meridional da plataforma sul-americana. *Rev. Bras. Geoc.*, **13**:139-158.

Almeida F.F.M. & Carneiro C.D.R. 1998. Origem e evolução da Serra do Mar. *Rev. Bras. Geoc.*, **28**:135-150.

Alves F.R. & Gomes C.B. 2001. Ilha dos Búzios, Litoral Norte do Estado de São Paulo: aspectos geológicos e petrográficos. *Geologia USP*, *Sér. Cient.*, **1**:101-114.

Amaral G., Bushee J., Cordani U.G., Kawashita H., Reynolds J.H. 1967. Potassium-argon ages of alkalines rocks from southern Brazil. *Geoch. Cosmoch. Acta*, **31**:117-142.

Azzone R.G., Ruberti E., Enrich G.E.R., Alves F.R. 2004. Aspectos geológicos do complexo alcalino máfico-ultramáfico de Ponte Nova, SP. *In:* SBG, Congresso Brasileiro de Geologia, 42, Araxá, *Anais*. CD-ROM.

Bellieni G., Montes Lauar C.R., De Min A., Piccrillo E. M., Cavazzini G., Melfi A.J., Pacca I.G. 1990. Early and late cretaceous magmatism from São Sebastião Island (SE - Brazil): Geochemistry and petrology. *Geochim. Brasil.,* **4**:59-83.

Bjornberg A.J.S. & Ellert R. 1955. Observações Geológicas e Petrológicas sobre a Ilha dos Búzios. *An. Acad. Bras. Ciênc.,* **27**:169-182.

Brown W.L. 1993. Fractional crystallization and zoning in igneous feldspars: ideal water-buffered liquid fractionation lines and feldspar zoning paths. *Contrib. Mineral. Petrol.,* **113**:115-125.

Chayes F. 1977. The oceanic basalt-trachyte relation in general and in the Canary Islands. *Am. Mineral.*, **62**:666-671.

Comin-Chiaramonti P. & Gomes C.B. 2005. *Mesozoic to Cenozoic alkaline magmatism in the Brazilian Platform*. Edusp/Fapesp, São Paulo, 736p.

Comin-Chiaramonti P., Gomes C.B., Castorina F., Censi P., Antonini P., Furtado S., Ruberti E., Scheibe F. 2002. Geochemistry and geodynamic implications of the Anitápolis and Lages alkaline-carbonatite complexes, Santa Catarina State, Brazil. *Rev. Bras. Geoc*., **32**:43-58.

Comin-Chiaramonti P., Gomes C.B., Marques L.S., Censi P., Ruberti E., Antonini P. 2005. Carbonatites from southeastern Brazil: geochemistry, O-C, Sr-Nd-Pb isotopes and relationships with the magmatism from the Paraná-Angola-Namibia Province. *In*: Comin-Chiaramonti P. & Gomes C.B. (eds.). *Mesozoic to Cenozoic alkaline magmatism in the Brasilian Plataform*. Edusp/Fapesp, São Paulo, p. 651-682.

Coutinho J.M.V. & Ens H.H. 1992. Diques lamprofíricos e diferenciados carbonatíticos da região de São Sebastião e Itanhaém - SP (resultados preliminares). *In*: SBG, Congr. Bras. Geol., 37, São Paulo, *Bol. Resumos Expandidos,* v.1, p. 512-513.

Coutinho J.M.V. & Melcher G.C. 1973. Levantamento Geológico e Petrográfico da Ilha Monte de Trigo (litoral norte de São Paulo, Brasil). *Rev. Bras. Geoc.,* **3**:243-256.

Deer W.A., Howie R.A., Zussman J. 1992. *An Introduction to the Rock-Forming Minerals*. Second Edition. Longman Scientific & Tecnical, 696p.

Derby O.A. 1887. On nefelinic rocks in Brazil, with special reference to the association of phonolite and foyaite. *Quart. Jour. Geol. Soc.*, **43**:457-473.

Enrich G.E.R., Azzone R.G., Ruberti E., Gomes C.B., Comin-Chiaramonti P. 2005. Itatiaia, Passa Quatro and São Sebastião island, the major alkaline syenitic complexes from the Serra do Mar Region. *In*: Comin-Chiaramonti P.& Gomes C.B. (eds.) *Mesozoic to Cenozoic Alkaline Magmatism in the Brasilian Plataform*. Edusp/Fapesp, São Paulo, p. 419-442.

Ernesto M., Marques L.S., Piccirillo E.M., Molina E.C., Ussami N., Comin-Chiaramonti P., Bellieni G. 2002. Paraná Magmatic Province-Tristan da Cunha plume system: fixed versus mobile plume, petrogenetic considerations and alternative heat sources. *J. Vol. Geothem. Res.*, **118**:15-36.

Freitas R.O. 1947. Geologia e petrologia da Ilha de São Sebastião. *Bol. Fac. Fil. Ciênc. Let. USP*, **85**:1-244.

Garda G. & Schorscher J.H.D. 1996. Os diques costeiros básicos e ultrabásicos adjacentes ao canal de São Sebastião (Litoral Norte do Estado de São Paulo). *Rev. IG São Paulo*, **17**:7-31.

Garda G., Schorscher J.H.D., Esperança S., Carlson R.W. 1995. The Petrology and Geochemistry of Coastal Dikes from São Paulo State, Brazil: Implication for Variable Litospheric Contributions to Alkaline Magmas from the Western Margins of the South Atlantic. *An. Acad. Bras. Ci.,* **67**:191-216.

Gibson S.A., Thompson R.N., Leonardos O.H., Dickin A.P., Mitchell J.G., 1995. The Late Cretaceus impact of the Trindade Mantle Plume. Evidence from large-volume mafic, potassic magmatism in SE, Brazil. *J. Petrol.*, **36**:189-230.

Gomes C.B., Damasceno E.C., Melcher G.C., Born H. 1967. Observações geológicas preeliminares sobre a Ilha de Vitória, SP. *Bol. Paran. Geoc.*, **26**:334-346.

Gomes C.B., Ruberti, E., Morbidelli, L. 1990. Carbonatite complexes from Brazil: a review. *J. South Am. Earth Sci.*, **3**:51-63.

Hamilton D.L. & Mackenzie W.S. 1965. Phase equilibria studies in the system NaAlSiO4 (nepheline) - KAlSiO4 (kalsilite) - SiO2 - H2O. *Mineral. Mag*., **34**:214-231.

Heilbron M., Pedrosa-Soares A.C., Campos Neto M.C., Silva L.C., Trouw R.A.J., Janasi V.A. 2004. Província Mantiqueira. *In:* Mantesso Neto V., Bartorelli A., Dal Ré Carneiro C., Brito Neves B.B. de (eds). *Geologia do Continente Sul-Americano: Evolução da Obra de Fernando Flávio Marques de Almeida*, Beca, São Paulo. p. 203-234.

Hennies W.T. & Hasui Y. 1977. Contribuição ao reconhecimento da geologia da Ilha de São Sebastião. *In:* SBG, Simpósio de Geologia Regional, 1, São Paulo, *atas*, p. 199-209.

Le Maitre R.W. (ed.) 2002. *Igneous rocks. A classification of igneous rocks and glossary of terms.* 2nd edition. Cambridge, Cambridge University Press, 236p.

Lima G.A. 2001. *Gabros estratiformes da região norte da Ilha de São Sebastião, SP*. Dissertação de Mestrado, Instituto de Geociências, Universidade de São Paulo, 170p.

Machado N., Valladares C., Heilbron M., Valeriano C. 1996. U-Pb geochronology of the central Ribeira belt (Brazil) and implications for the evolution of the Brazilian Orogeny. *Precambrian Research,* **79**:347-361.

Mackenzie W.S., Donaldson C.H., Guilford C. 1993. *Atlas of igneous rocks and their textures.* Longman Scientific & Tecnical, 148p.

McBirney A.R. 1996. The Skaergaard Intrusion. *In:* Cawthorn (ed.) *Layered Intrusions.* Developments in Petrology 15, Elsevier Science, p. 147-180.

Montes-Lauar C.R., Pacca I.G., Melfi A.J., Kawashita K. 1995. Late Cretaceous alkaline complexes, southeastern Brazil: paleomagnetism and geochronology. *Earth Planet. Sci. Lett.*, **134**:425-440.

Morbidelli L., Gomes C.B., Beccaluva L., Brotzu P., Conte A.M., Ruberti E., Traversa G. 1995. Mineralogical, petrological and geochemical aspects of alkaline and alkaline-carbonatite associations from Brazil. *Earth Sci. Rev*., **39**:135-168.

Motoki A. & Gomes C.B. 1984. Caracterização geológica e petrológica do maciço alcalino da Ilha de Vitória, SP. *In:* SBG, Congresso Brasileiro de Geologia, 34, Rio de Janeiro, *anais*, v. 9, p. 4392-4399.

Myers J.S. 1976. Channel deposits of peridotite, gabbro and chromitite from turbidity currents in the stratiform Fiskenaesset anorthosite complex, Southwest Greenland. *Lithos,* **9**:281-291.

Parsons I. & Becker S. 1987. Layering, Compaction and Post-Magmatic Processes in the Klokken Intrusion. *In:* Parsons I. (ed.) *Origins of Igneous Layering*. D. Reidel Publishing Company, p. 29-92.

Riccomini C., Velázquez V.F., Gomes C.B. 2005. Tectonic controls of the Mesozoic and Cenozoic alkaline magmatism in Central-Southeastern Brazilian Platform. *In:* Comin-Chiaramonti P. & Gomes C.B. (eds.) *Mesozoic to Cenozoic Alkaline Magmatism in the Brazilian Platform*. Edusp/Fapesp, São Paulo, p. 31-55.

Rickwood P.C. 1990. The anatomy of a dyke and the determination of propagation and magma flow directions. *In:* Parker, Rickwood & Tucker (eds.). *Mafic Dykes and Emplacement Mechanisms.* Rotterdam, Balkema, p. 81-100.

Rock N.M.S. 1991. *Lamprophyres.* Blackie/Van Nostand Reinhold, 285p.

Smith A.D. & Lewis C. 1999. The planet beyond the plume hypothesis. *Earth Sci. Rev.*, **48**:135-182.

Sonoki I.K. & Garda G.M. 1988. Idades K-Ar de rochas alcalinas do Brasil Meridional e Paraguai Oriental: compilação e adaptação às novas constantes de decaimento. *Bol. IG-USP*, **19**:63-85.

Thompson R.N., Gibson S.A., Mitchell J.G., Dickin A.P., Leonardos O.H., Brod J.A., Greenwood J.C. 1998. Migrating Cretaceous-Eocene magmatism in the Serra do Mar Alkaline Province, SE Brasil: melts from the deflected Trindade Mantle Plume? *J. Petrol.*, **39**:1493-1526.

Tröger W.E. 1979. *Optical determination of rock-forming minerals*. E. Schweizerbart' Scheverlagsbuchhandlung, 188p.

Ulbrich H.H.G.J. & Gomes C.B. 1981. Alkaline Rocks From Brazil. *Earth Sci. Rev.*, **17**:135-154.

Ulbrich H.H.G.J., Garda G.M., Ulbrich M.N.C. 1991. Avaliação das idades K-Ar dos maciços alcalinos do Brasil sul-oriental e do Paraguai oriental. *Bol. IG-USP Série especial*, **9**:87-92.

Vandecar J.C., James D.E., Assumpção M. 1995. Seismic evidence for a fossil mantle plume beneath South America and implications for plate driving forces. *Nature*, **378**:25-31.

Vasconcelos P.M., Onoe A.T., Kawashita K., Soares A.J., Teixeira W. 2002. $^{40}Ar/^{39}Ar$ geochronology at the Instituto de Geociências, USP: instrumentation, analytical procedures, and calibration. *An. Acad. Bras. Ci.,* **74**:297-342.

Wager L.R. & Brown G.M. 1968. *Layered igneous rocks*. San Francisco, W. H. Freeman, 588 p.

Williams H., Turner F.J., Gilbert C.M. 1982. *Petrography - An Introduction to the Study of Rocks in Thin Sections*. Second Edition. New York, W.H. Freeman and Company, 626p.

Manuscrito ID 10469
Submetido em 31 de janeiro 2008
Aceito em 13 de fevereiro de 2009